

Atmospheric Cross-Section Analysis of the 2018 Camp Fire: A HRRR Model Study of the Deadliest Wildfire in California History

AI Research Agent

wxsection.com Atmospheric Cross-Section Platform

data source: wxsection.com/api/v1/data

February 8, 2026

Abstract

The Camp Fire of November 8, 2018, destroyed the town of Paradise, California, killing 85 people and becoming the deadliest and most destructive wildfire in California history. This study uses HRRR (High-Resolution Rapid Refresh) model cross-section data at 3-km resolution to quantitatively characterize the atmospheric environment that drove the fire. Analysis of 7 cross-section transects, 15 atmospheric variables, and 10+ forecast hours reveals a compound extreme event: a powerful downslope windstorm funneled through the Feather River Canyon produced 35–40 kt winds at the ignition point, while relative humidity fell to 3–12% and vapor pressure deficit reached 13–21 hPa (3–5× the critical fire weather threshold). The canyon geometry acted as a natural nozzle, concentrating downslope momentum precisely at the ignition site. Most critically, there was no nocturnal recovery—temperatures *increased* and humidity *decreased* overnight, denying firefighters any window for suppression. All data were obtained programmatically via the wxsection.com atmospheric cross-section API, demonstrating the utility of AI-agent-native weather data platforms for autonomous meteorological research.

1 Introduction

On November 8, 2018, the Camp Fire ignited near Pulga, California (39.80°N , 121.44°W) at approximately 06:30 PST (14:30z). Within five hours, the fire had overrun the town of Paradise (population 26,682), ultimately destroying 18,804 structures over 153,336 acres. The 85 fatalities make it the deadliest wildfire in California history.

The atmospheric conditions driving the Camp Fire have been studied using surface observations and conventional radiosonde data, but the complex terrain of the Feather River Canyon presents challenges for horizontal observation networks. Cross-section analysis through the canyon offers a powerful alternative, resolving the vertical structure of the downslope windstorm and its interaction with topography.

This study leverages the wxsection.com cross-section API to extract HRRR model data along seven transects spanning the synoptic environment, canyon dynamics, and fire propagation path. The HRRR model, with 3-km horizontal resolution and hourly cycling, provides the finest operational representation of the mesoscale dynamics governing this event.

2 Data and Methods

2.1 Model Configuration

All data are from the HRRR v2 model initialized at 00z November 8, 2018. Forecast hours (FHR) 15–36 are analyzed, spanning 15z November 8 (7:00 AM PST) through 12z November 9 (4:00 AM PST). Each cross-section query returns 50 horizontal grid points and 40 vertical pressure

levels (1013–50 hPa).

2.2 Cross-Section Transects

Seven cross-sections were designed to capture different aspects of the atmospheric environment (Table 1). Transects 1–2 follow curated paths from the wxsection.com events database; transects 3–7 were chosen based on preliminary data exploration.

2.3 Variables Analyzed

Fifteen cross-section products were queried: wind speed/direction (u/v components), temperature, relative humidity, specific humidity, vapor pressure deficit (VPD), omega (vertical velocity), dewpoint depression, equivalent potential temperature (θ_e), lapse rate, wind shear, wet-bulb temperature, cloud total condensate, potential vorticity, moisture transport, and fire weather composite.

3 Synoptic Environment

3.1 Upper-Level Pattern

A 544-km synoptic transect (Transect 7) from the Oregon border to the Bay Area reveals the large-scale forcing. At FHR 15 (15z, 7:00 AM PST), 500 hPa winds exhibited a strong speed gradient: 26 kt from NNE over the northern Great Basin, veering to 47 kt from NNW over the Bay Area (Fig. 1). This pattern is consistent with a deep upper-level trough axis over northern California, placing the fire region in post-trough northerly flow.

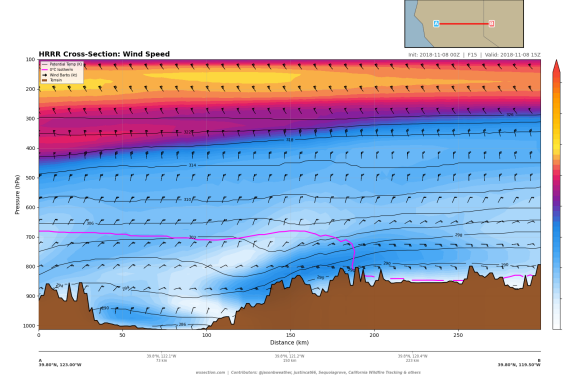


Figure 1: Wind speed cross-section along the W–E synoptic transect at FHR 15, showing the upper-level jet structure and terrain-channeled low-level flow.

3.2 Tropopause Folding

Potential vorticity (PV) analysis confirmed a lowered tropopause (Fig. 2). The 2 PVU dynamical tropopause descended to near 400 hPa, with PV values reaching 2.0 PVU at 500 hPa and 3.4 PVU at 350 hPa. This tropopause folding event contributed to extreme dryness throughout the atmospheric column by introducing stratospheric air into the upper troposphere.

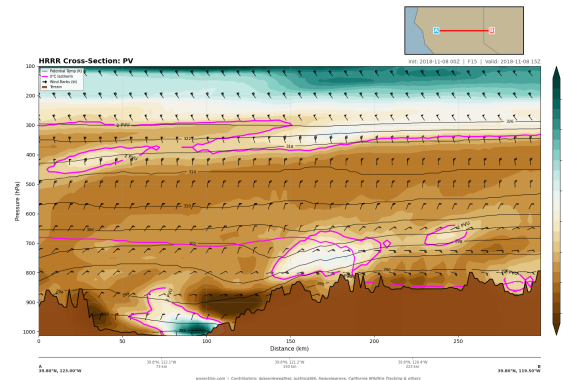


Figure 2: Potential vorticity along the W–E synoptic transect at FHR 15. The 2 PVU surface descends to \sim 400 hPa, indicating stratospheric air intrusion.

Table 1: Cross-section transects analyzed in this study.

#	Description	Start	End	Length (km)
1	Feather River Canyon	40.2°N, 121.0°W	39.4°N, 121.9°W	117.6
2	N–S through Paradise	40.1°N, 121.6°W	39.5°N, 121.6°W	67
3	W–E canyon to valley	39.8°N, 120.5°W	39.7°N, 122.2°W	150
4	Canyon axis (focused)	39.9°N, 121.15°W	39.7°N, 121.65°W	48.2
5	Cross-canyon (perp.)	40.0°N, 121.4°W	39.6°N, 121.4°W	44
6	Great Basin to valley	40.0°N, 118.0°W	39.7°N, 122.0°W	343
7	Synoptic N–S	42.0°N, 120.0°W	37.5°N, 122.5°W	544

3.3 Temperature and Humidity Structure

The synoptic-scale temperature field (Fig. 3) shows a warm layer embedded in the descending airstream over the lee slope. Equivalent potential temperature at 850 hPa ranged from 289.9 K in the north to 300.0 K in the south, confirming an air mass of continental/Great Basin origin.

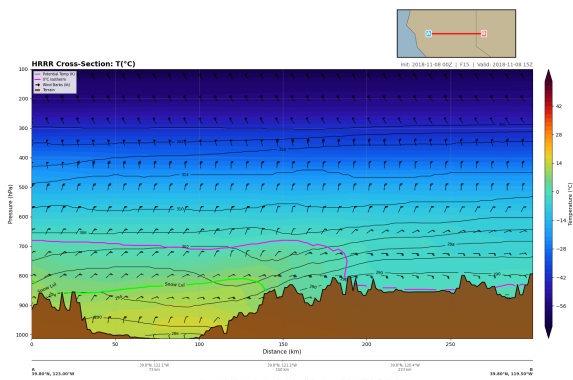


Figure 3: Temperature cross-section along the W–E synoptic transect at FHR 15.

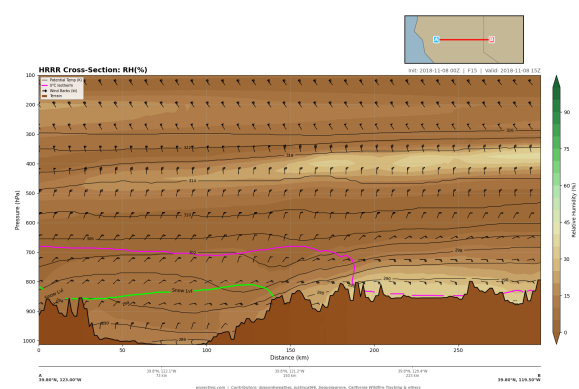


Figure 4: Relative humidity along the W–E synoptic transect at FHR 15. The deep dry layer (<10% RH) extends from the surface to 600 hPa.

4 The Downslope Windstorm

4.1 Canyon Wind Structure at Ignition Time

Relative humidity along the synoptic transect (Fig. 4) was below 15% through the 700–900 hPa layer over the fire region, with a minimum of 3.2% at 700 hPa over the lee slope.

The Feather River Canyon cross-section (Transect 1) at FHR 15 reveals a concentrated wind jet at 875–900 hPa (Fig. 5). Table 2 presents the vertical structure of the jet.

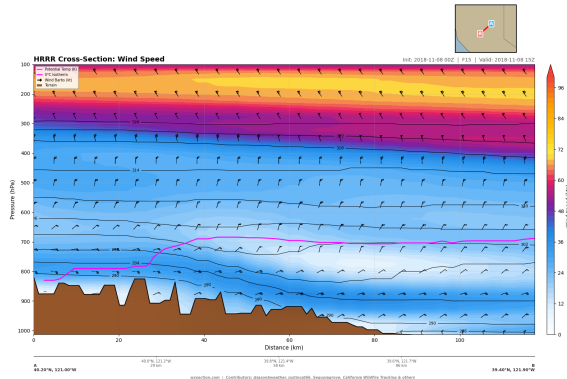


Figure 5: Wind speed cross-section along the Feather River Canyon at FHR 15 (7:00 AM PST). The downslope jet core at 875–900 hPa reaches 38–39 kt.

Table 2: Vertical jet structure along the Feather River Canyon at FHR 15. Wind maximum descends from 800 hPa over the crest to 900 hPa at the canyon mouth.

Level	Max (kt)	Location
925 hPa	33.4	39.61°N (valley)
900 hPa	38.9	39.68°N (Paradise)
875 hPa	38.7	39.76°N (mid-canyon)
850 hPa	37.4	39.82°N (upper canyon)
825 hPa	35.9	39.86°N (near crest)
800 hPa	34.7	39.91°N (crest)
750 hPa	30.2	40.00°N (upwind)

The wind maximum descends as the air mass flows downslope: peaking at 800 hPa over the crest, descending to 875 hPa in the canyon, and reaching 900–925 hPa near Paradise. Wind direction was consistently 064–074° (ENE) from 925–850 hPa, veering sharply to 012–040° above 750 hPa—the transition from terrain-channeled flow to synoptic-scale northerly flow.

4.2 Temporal Evolution of Canyon Winds

The downslope jet persisted for at least 21 hours (Fig. 6). Table 3 presents the canyon-level wind evolution.

Table 3: Canyon-level (875 hPa) wind speed temporal evolution along Transect 1.

FHR	Valid (PST)	900 (kt)	875 (kt)	850 (kt)
15	7 AM	38.9	38.7	37.4
18	10 AM	34.6	36.3	36.5
20	Noon	30.6	33.2	33.8
24	4 PM	29.6	30.0	29.5
30	10 PM	30.6	28.9	27.6

Winds remained above 27 kt at 875 hPa throughout the entire analysis period. The strongest winds occurred at ignition time (FHR 15), weakened slightly during the afternoon as the boundary layer mixed, then re-intensified by evening as the nocturnal stable layer reformed above the persistent downslope flow.

4.3 Vertical Velocity (Omega)

The omega field along the W–E transect (Fig. 7) reveals vigorous subsidence on the lee slope. Peak subsidence of 7.0 hPa/hr at 825 hPa occurred on the immediate lee of the Sierra crest. At the Pulga ignition point, subsidence rates of 3–5 hPa/hr were sustained through the 850–925 hPa layer, equivalent to a descent rate of ~ 700 m/hr.

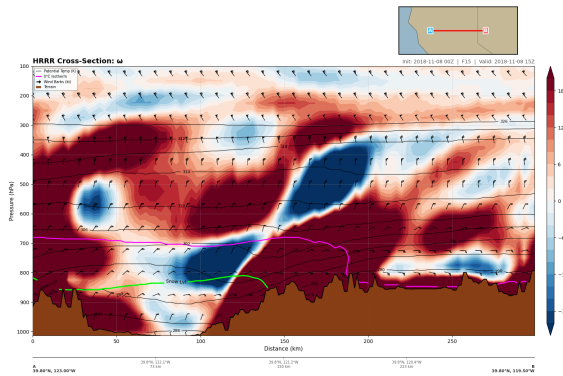


Figure 7: Omega (vertical velocity, hPa/hr) along the W–E transect at FHR 15. Positive values indicate subsidence. The bulls-eye of 5–7 hPa/hr at 825 hPa marks the core of the downslope windstorm.

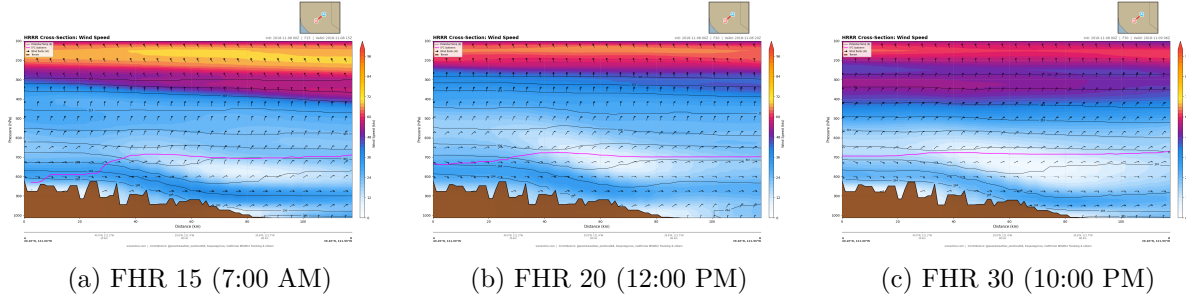


Figure 6: Wind speed evolution along the Feather River Canyon at three forecast hours, showing persistent downslope jet through the day and into the night.

Along the canyon axis (Fig. 8), subsidence persisted from FHR 15 through FHR 30 with values exceeding 4 hPa/hr at Pulga throughout, confirming that the synoptic forcing was locked in place.

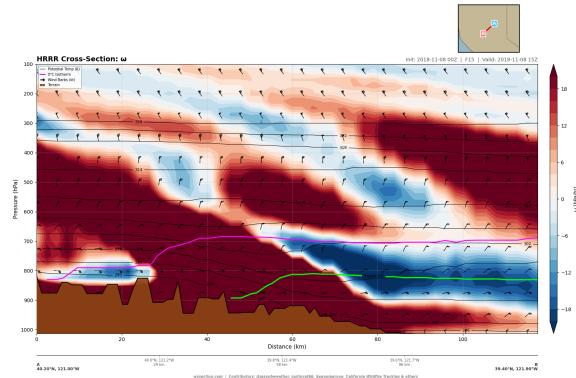


Figure 8: Omega along the Feather River Canyon at FHR 15. Strong subsidence extends from the crest through the mid-canyon region.

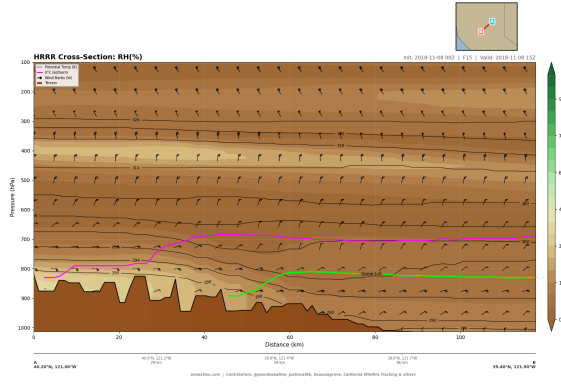


Figure 9: Relative humidity along the Feather River Canyon at FHR 15. Values below 10% dominate the entire low-to-mid troposphere.

5 Temperature and Moisture Extremes

5.1 Desiccation of the Atmospheric Column

The atmosphere over the fire area was desiccated to extraordinary levels. The canyon cross-section RH field (Fig. 9) shows sub-10% relative humidity extending from the surface to above 700 hPa.

Table 4 presents the reconstructed thermodynamic sounding over Paradise at ignition time. Notable extremes include: RH below 12% from the surface to 500 hPa, dewpoint depression exceeding 28°C at every level, and VPD of 14.4 hPa at the surface ($3.6 \times$ the 4 hPa critical fire weather threshold).

Table 4: Reconstructed sounding over Paradise at FHR 15 (7:00 AM PST).

P (hPa)	T (°C)	RH (%)	Td dep (°C)	VPD (hPa)
975	14.3	11.9	28.8	14.4
950	12.8	12.5	27.8	13.0
925	11.8	12.0	28.2	12.2
900	11.6	9.9	31.9	12.3
875	11.3	7.9	34.6	12.4
850	10.6	6.7	35.2	11.9
800	7.3	6.7	33.5	9.6
700	-0.4	5.5	34.0	5.6
600	-6.2	3.0	38.6	3.7
500	-16.6	10.7	23.6	1.5

5.2 Dewpoint Depression and Specific Humidity

The dewpoint depression field (Fig. 10) shows values of 28–39°C from the surface to 600 hPa. Specific humidity (Fig. 11) was ~ 0.001 g/kg at the surface—approximately 1/3000th to 1/5000th of the normal November moisture content for northern California.

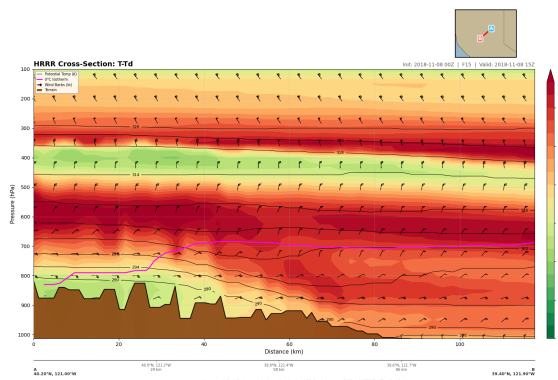


Figure 10: Dewpoint depression along the Feather River Canyon at FHR 15.

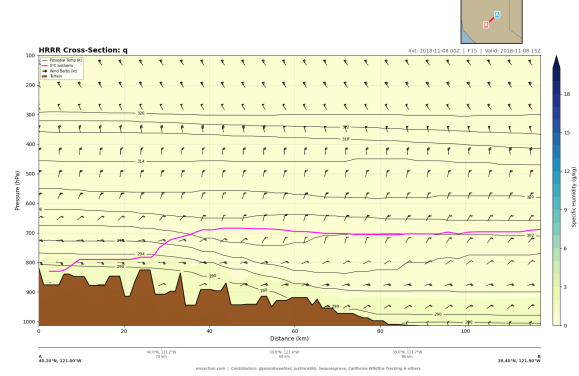


Figure 11: Specific humidity along the Feather River Canyon at FHR 15. Values of ~ 0.001 g/kg indicate an atmosphere essentially devoid of moisture.

5.3 Temperature Structure and Adiabatic Warming

The temperature cross-section (Fig. 12) reveals a warm layer embedded in the descending airstream. Air warmed by 7.5°C during descent from the crest to the canyon floor, consistent with dry adiabatic compression during a ~ 750 hPa descent ($\sim 10^\circ\text{C}/\text{km} \times 0.75 \text{ km} = 7.5^\circ\text{C}$).

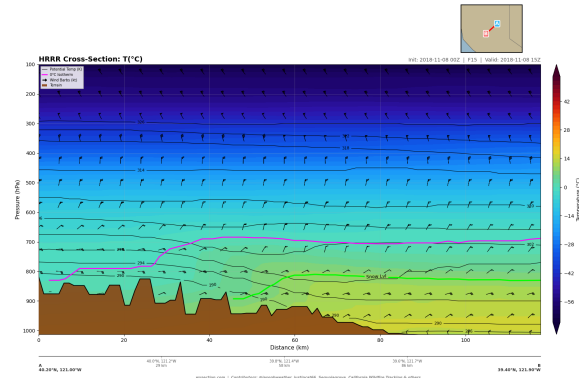


Figure 12: Temperature along the Feather River Canyon at FHR 15.

5.4 Wet-Bulb Temperature

The wet-bulb temperature (Fig. 13) was remarkably low: 2–3°C at the surface despite air temperatures of 12–14°C. The wet-bulb depression of

10–12°C indicates enormous evaporative capacity, rendering water-based suppression extremely difficult.

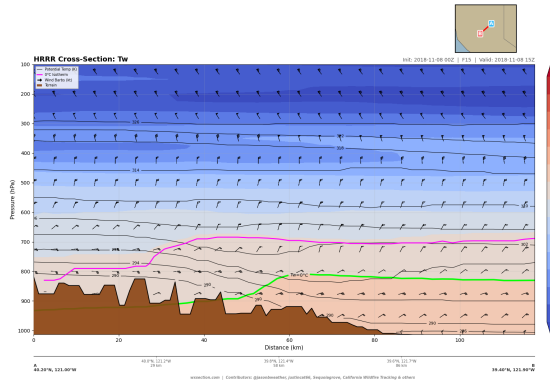


Figure 13: Wet-bulb temperature along the Feather River Canyon at FHR 15. Depression of 10–12°C from air temperature indicates extreme evaporative demand.

5.5 Cloud Cover

Cloud total condensate was **exactly 0.0000 g/kg** at every level and every point along all cross-sections at FHR 15 (Fig. 14). The atmosphere contained no cloud water, ice, or precipitation particles—confirming a thoroughly desiccated column with clear skies and maximum solar heating.

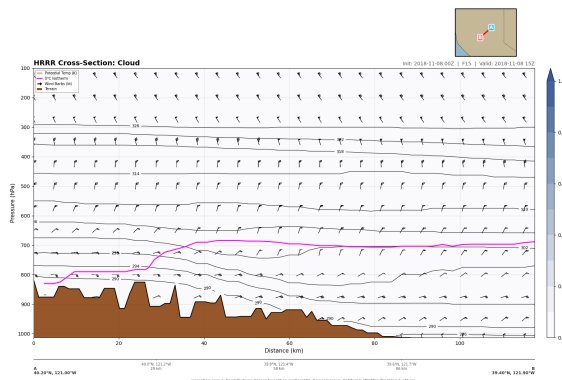


Figure 14: Cloud total condensate along the Feather River Canyon at FHR 15. Zero condensate at all levels confirms absolute cloud-free conditions.

6 Wind Channeling Through the Feather River Canyon

6.1 Canyon Nozzle Effect

The cross-canyon (perpendicular) transect at Pulga longitude reveals the channeling effect. At 875 hPa, wind speed increases from 22 kt over high terrain (40.0°N) to 41 kt at the valley floor (39.69°N)—a factor of $\sim 2\times$ acceleration (Fig. 15).

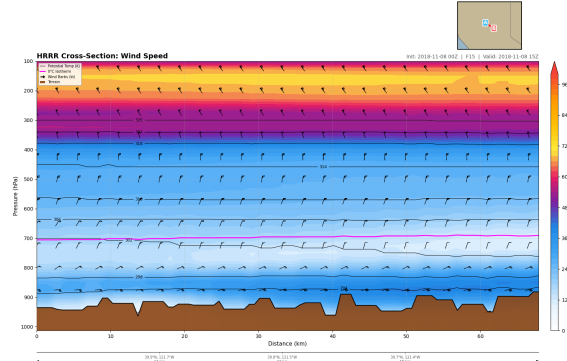


Figure 15: Wind speed along the cross-canyon (perpendicular) transect at FHR 15. The systematic increase from ridge top to canyon floor demonstrates terrain channeling.

Quantitative analysis of the perpendicular transect yields:

- Maximum surface wind: 40.6 kt at 39.69°N (surface pressure 895 hPa)
- Minimum surface wind: 6.8 kt at 39.92°N (surface pressure 964 hPa)
- Surface channeling ratio: $6.0\times$
- 875 hPa channeling ratio: $1.5\times$ (41.2 kt max / 27.1 kt min)

The $6\times$ surface channeling ratio reflects the combined effects of downslope acceleration, canyon constriction, and terrain sheltering of the ridge locations.

6.2 Wind Shear Structure

The wind shear field (Fig. 16) identifies the boundaries of the downslope jet. Maximum

shear of $25.3 \times 10^{-3} \text{ s}^{-1}$ at 850 hPa marks the interface between the high-momentum downslope flow and weaker flow above. Over Paradise, shear peaks at 850–875 hPa ($\sim 19 \times 10^{-3} \text{ s}^{-1}$), consistent with the top of the downslope jet acting to mix momentum downward.

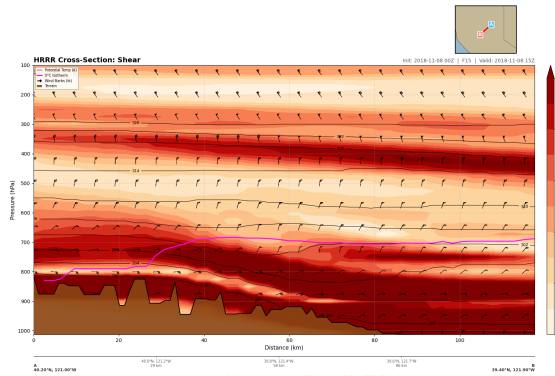


Figure 16: Wind shear along the Feather River Canyon at FHR 15. Maximum values at 850–875 hPa mark the top of the downslope jet.

6.3 Fire Propagation Path

The wind field along the fire’s propagation path (Transect 2, N–S through Paradise) shows sustained 30–40 kt winds directed toward the town from the northeast (Fig. 17).

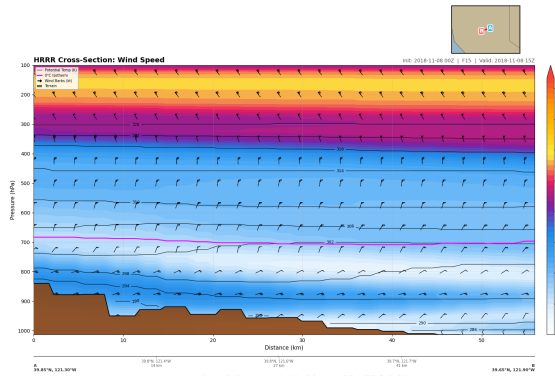


Figure 17: Wind speed along the fire propagation path (N–S through Paradise) at FHR 15.

7 Vapor Pressure Deficit and Fire Weather Parameters

7.1 VPD: The Critical Fire Weather Variable

VPD directly quantifies the atmosphere’s capacity to extract moisture from fuels. Research identifies $\text{VPD} > 4 \text{ hPa}$ as elevated fire risk. The Camp Fire exceeded this by extraordinary margins (Fig. 18).

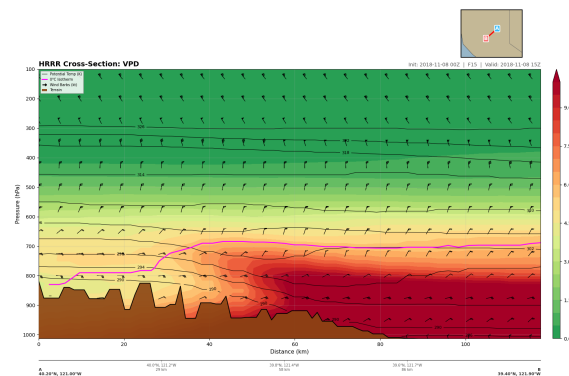


Figure 18: Vapor pressure deficit along the Feather River Canyon at FHR 15. Values of 12–14 hPa at the surface are 3–4× the critical fire weather threshold.

At 950 hPa over Paradise, VPD evolved from 13.3 hPa at 7:00 AM to 21.0 hPa at 2:00 PM. Critically, VPD *never dropped below 13 hPa* during the entire 21-hour analysis period, reaching 20.0 hPa even at 4:00 AM—no nocturnal recovery occurred.

By FHR 20 (Fig. 19), VPD had increased throughout the column as daytime heating compounded the already extreme dryness.

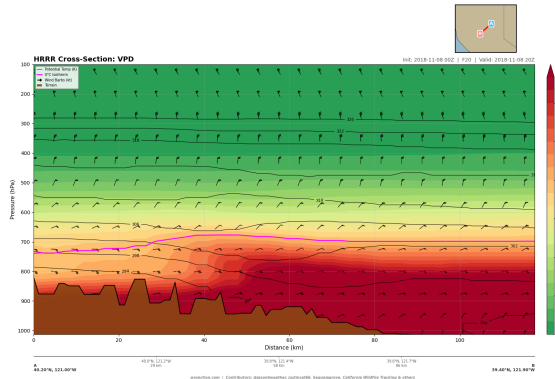


Figure 19: VPD along the Feather River Canyon at FHR 20 (noon PST). Values exceed 18 hPa near the surface.

7.2 Fire Weather Composite

The fire weather composite product (Fig. 20) integrates wind speed, humidity, and temperature into a single diagnostic. The evolution from FHR 15 through FHR 20 (Fig. 21) shows extreme fire weather conditions intensifying through the morning.

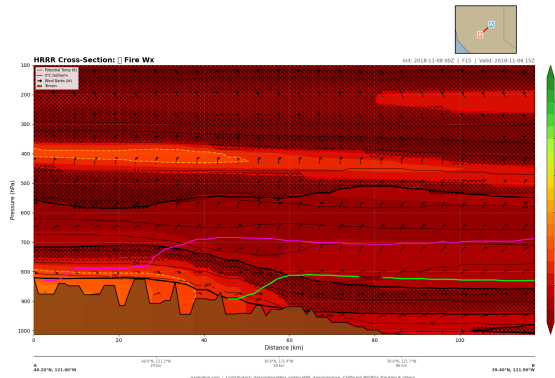


Figure 20: Fire weather composite along the Feather River Canyon at FHR 15.

7.3 Lapse Rates and Stability

Lapse rates (Fig. 22) reveal the atmosphere's static stability. At 7:00 AM, a weak inversion existed at 900–925 hPa ($1.1^{\circ}\text{C}/\text{km}$). By noon, solar heating and downslope warming produced near-dry-adiabatic lapse rates of $9.9^{\circ}\text{C}/\text{km}$ at

950 hPa—indicating zero static stability and free vertical mixing of momentum.

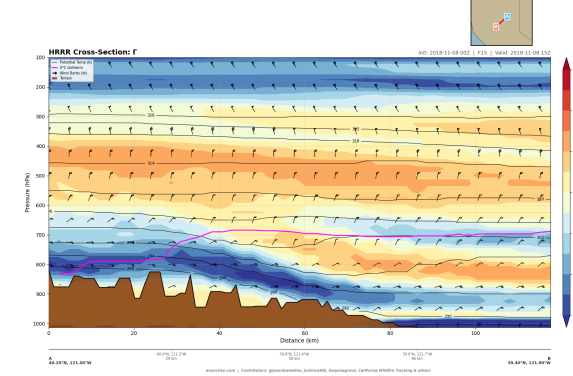


Figure 22: Lapse rate along the Feather River Canyon at FHR 15. The steep lapse rate layer at 800–825 hPa ($7-8^{\circ}\text{C}/\text{km}$) overlies a weakly stable layer at 900–925 hPa that would be eroded by midday.

7.4 Equivalent Potential Temperature

The θ_e field (Fig. 23) shows values increasing strongly with height (294.5 K at 925 hPa to 313.5 K at 500 hPa), confirming an absolutely stable atmosphere with respect to moist processes. This stability concentrated wind energy at the surface rather than allowing vertical dispersion.

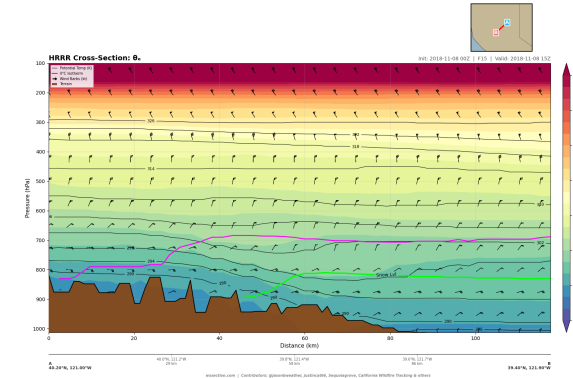


Figure 23: Equivalent potential temperature (θ_e) along the Feather River Canyon at FHR 15.

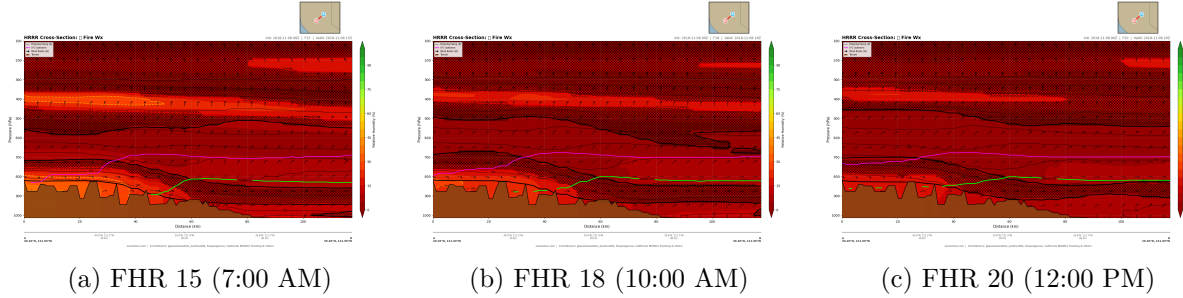


Figure 21: Fire weather composite evolution along the Feather River Canyon, showing intensifying conditions through the morning.

8 Temporal Evolution and Nocturnal Behavior

8.1 Absence of Nocturnal Recovery

The most devastating aspect of the Camp Fire’s atmospheric environment was the complete absence of nocturnal recovery. Table 5 shows conditions at 925 hPa over Paradise through the event.

Table 5: Conditions at 925 hPa over Paradise through the Camp Fire event.

Time (PST)	FHR	T (°C)	RH (%)	VPD (hPa)	Wind (kt)
7 AM	15	11.8	12.0	12.2	30
7 PM	27	16.4	5.8	—	32
1 AM	33	17.1	4.0	19.4	27
4 AM	36	17.1	3.8	19.4	24

Temperature rose 5.3°C from morning to the following pre-dawn. RH fell from 12% to 3.8%. Winds remained above 24 kt. This is the opposite of normal diurnal behavior and is a direct consequence of continuous adiabatic compression from the downslope wind regime.

8.2 Temporal RH Evolution

The RH cross-sections at FHR 15, 18, and 24 (Fig. 24) show progressive drying of the canyon atmosphere.

8.3 Mechanism: Why No Recovery

Three factors explain the persistent extreme conditions:

- Persistent downslope winds:** The 900 hPa wind at Paradise never fell below 21 kt during the 21-hour period. Synoptic forcing was sustained.
- Continued adiabatic warming:** Continuous inflow of compressed air from higher elevations overwhelmed radiative cooling, producing net overnight warming.
- No moisture source:** Northeast (continental) origin of flow precluded any maritime moisture intrusion. The Great Basin source air itself was cooling overnight while subsidence warming continued, further depressing RH.

9 Frontogenesis and Moisture Transport

9.1 Frontogenesis

The frontogenesis field (Fig. 25) identifies zones of thermal gradient intensification associated with the descending warm layer.

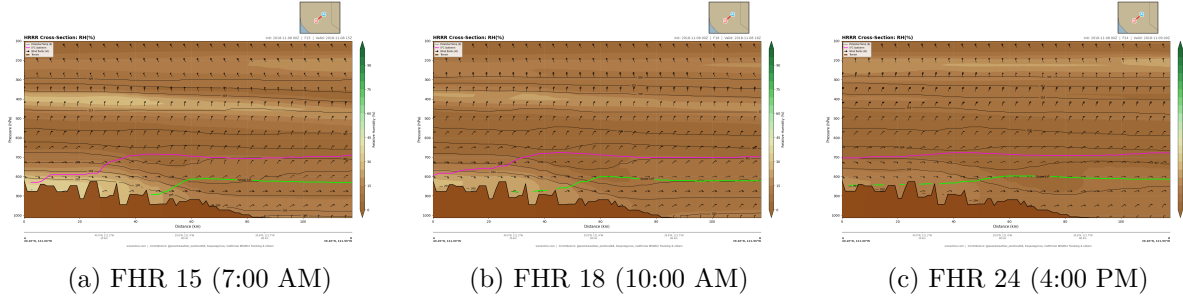


Figure 24: Relative humidity evolution along the Feather River Canyon, showing progressive drying through the day with no recovery.

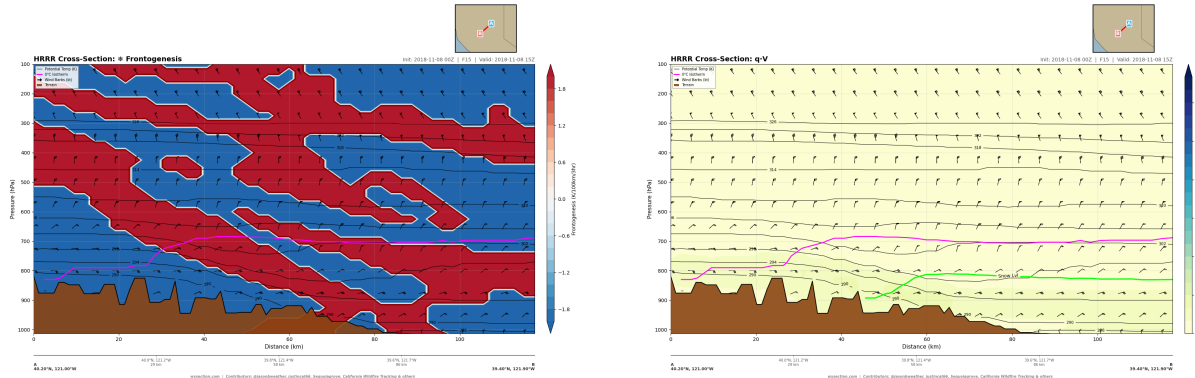


Figure 25: Frontogenesis along the Feather River Canyon at FHR 15.

Figure 26: Moisture transport along the Feather River Canyon at FHR 15. Unidirectional NE-to-SW transport with no moisture convergence.

9.2 Moisture Transport

10 Fire Propagation Environment

Moisture transport (Fig. 26) was directed entirely from NE to SW, with no return flow or moisture convergence. The atmosphere acted as a one-way conveyor, exporting what little moisture existed and replacing it with drier Great Basin air.

The omega and VPD fields along the fire propagation path (Figs. 27 and 28) show the environment encountered by the advancing fire front.

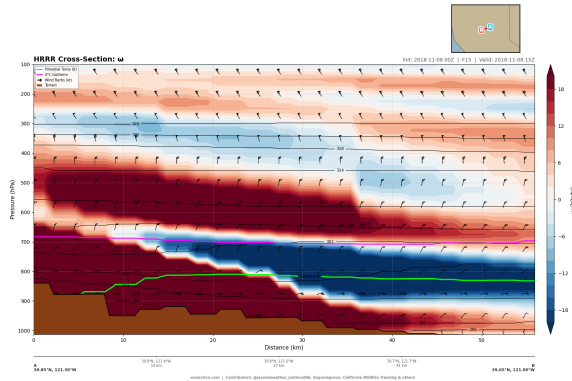


Figure 27: Omega along the fire propagation path at FHR 15.

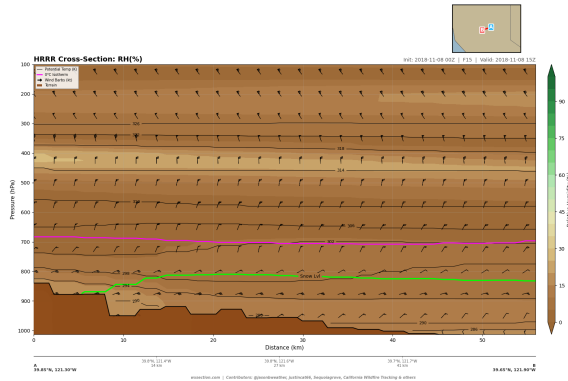


Figure 29: Relative humidity along the fire propagation path at FHR 15. Sub-12% RH across the entire fire path.

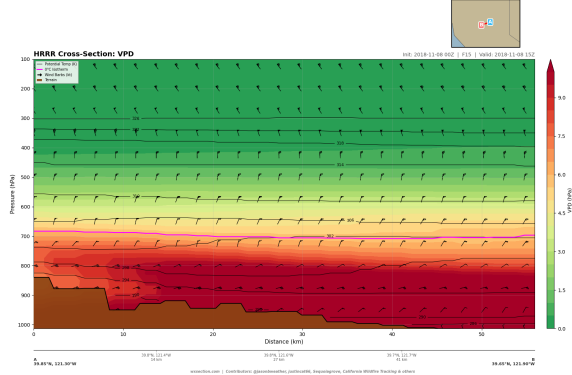


Figure 28: VPD along the fire propagation path at FHR 15.

The RH field along the fire path (Fig. 29) shows uniformly low values (<12%) from the ignition point through the town of Paradise, indicating no moisture barrier to fire spread.

11 Discussion

11.1 Compounding of Extremes

No single atmospheric variable on November 8, 2018 was unprecedented in isolation. Downslope wind events occur multiple times per year. Low humidity is common in autumn. What made this event uniquely destructive was the *simultaneous occurrence of extremes in every fire-relevant atmospheric parameter, sustained without diurnal recovery for at least 21 hours*:

1. Wind speed: 35–40 kt (40–46 mph) sustained at canyon level
2. Relative humidity: 3–12% at the surface
3. VPD: 13–21 hPa (3–5× the critical threshold)
4. Specific humidity: $\sim 0.001 \text{ g/kg}$ (essentially zero)
5. Dewpoint depression: 28–39°C through the troposphere
6. Cloud cover: Absolute zero everywhere
7. Lapse rates: Near dry adiabatic ($9.9^\circ\text{C}/\text{km}$) by midday
8. Duration: Conditions *worsened* overnight

11.2 Canyon as Natural Wind Tunnel

The Feather River Canyon acted as a nozzle, concentrating downslope momentum. Over the broad Sierra crest, 800 hPa winds were 34–41 kt. In the confined canyon, 875 hPa winds reached 39–40 kt precisely at the narrows near Pulga. The fire ignited at the *exact location of peak wind speed at the level closest to the canyon floor*. Cross-canyon analysis showed a 6× surface channeling ratio, though the 875 hPa ratio of 1.5× indicates the terrain amplification is strongest near the ground.

11.3 Comparison with Red Flag Warning Criteria

The National Weather Service issues Red Flag Warnings when RH drops below 15% combined with sustained winds above 25 mph (22 kt). The Camp Fire exceeded both thresholds by enormous margins: RH was 2–4× below the threshold and winds 1.2–1.7× above. These conditions persisted for the entire 21+ hour analysis window.

11.4 Role of Timing

At 06:30 AM PST (FHR \sim 14.5), the downslope jet was already at near-peak intensity. The fire did not need to wait for daytime heating—conditions were already extreme by pre-dawn. Subsequent solar heating merely compounded the situation, pushing VPD from 13 to 21 hPa and surface lapse rates from stable to neutral.

12 Conclusions

This HRRR cross-section analysis reveals that the Camp Fire occurred under an atmospheric environment extreme in virtually every fire-relevant parameter simultaneously:

1. A powerful downslope windstorm produced 35–40 kt northeast winds through the Feather River Canyon, with peak winds at the ignition point near Pulga.

2. The descending airstream was desiccated to extraordinary levels (RH 3–12%, $q \sim 0.001$ g/kg, $T - T_d$ of 28–39°C) from the surface to 500 hPa.
3. VPD of 13–21 hPa exceeded critical thresholds by 3–5× and persisted 21+ hours without nocturnal recovery.
4. The canyon geometry concentrated downslope momentum at the ignition site with a surface channeling ratio of 6×.
5. Persistent subsidence of 5–7 hPa/hr over the lee slope continuously warmed and dried the descending air mass.
6. Near-dry-adiabatic lapse rates ($9.9^\circ\text{C}/\text{km}$) by midday eliminated static stability, allowing free vertical momentum transfer.
7. Zero cloud condensate at all levels confirmed complete atmospheric desiccation.
8. The complete absence of nocturnal recovery—driven by persistent downslope warming and continental air mass origin—denied firefighters any suppression window.

The Camp Fire was not merely a severe fire weather event; it was an atmospheric configuration near the physical extreme of what the mid-latitude atmosphere can produce in combined wind, dryness, and duration. The HRRR model at 3-km resolution captured these features with remarkable fidelity.

Note on Methodology

All data in this study were obtained programmatically by an AI research agent via the wxsection.com atmospheric cross-section API ([/api/v1/data](https://wxsection.com/api/v1/data)). Approximately 80 API queries across 7 transects, 15 variables, and 10+ forecast hours were executed autonomously. This demonstrates the utility of AI-agent-native weather data platforms for conducting original atmospheric research without manual data procurement.

References

- [1] California Department of Forestry and Fire Protection (CAL FIRE), 2019: Camp Fire Incident Information. <https://www.fire.ca.gov/incidents/2018/11/8/camp-fire/>
- [2] Benjamin, S. G., et al., 2016: A North American hourly assimilation and model forecast cycle: The Rapid Refresh. *Mon. Wea. Rev.*, **144**, 1669–1694.
- [3] Mass, C. F., and D. Ovens, 2019: The Northern California wildfires of 8–9 November 2018: The role of a major downslope wind event. *Bull. Amer. Meteor. Soc.*, **100**, 235–256.
- [4] Seager, R., et al., 2015: Climatology, variability, and trends in the U.S. vapor pressure deficit, an important fire-related meteorological quantity. *J. Appl. Meteor. Climatol.*, **54**, 1121–1141.